

# Anti-CD105 Antibody Eliminates Tumor Microenvironment Cells and Enhances Anti-GD2 Antibody Immunotherapy of Neuroblastoma with Activated Natural Killer Cells

Hong-Wei Wu<sup>1</sup>, Michael A. Sheard<sup>1</sup>, Jemily Malvar<sup>1</sup>, G. Esteban Fernandez<sup>1</sup>, Yves A. DeClerck<sup>1,2</sup>, Laurence Blavier<sup>1</sup>, Hiroyuki Shimada<sup>1,3</sup>, Charles P. Theuer<sup>4</sup>, Richard Sposto<sup>1,2</sup>, and Robert C. Seeger<sup>1,2</sup>



## Abstract

**Purpose:** We determined whether elimination of CD105<sup>+</sup> cells in the tumor microenvironment (TME) with anti-CD105 antibodies enhanced anti-disialoganglioside (GD2) antibody dinutuximab therapy of neuroblastoma when combined with activated natural killer (aNK) cells.

**Experimental Design:** The effect of MSCs and monocytes on antibody-dependent cellular cytotoxicity (ADCC) mediated by dinutuximab with aNK cells against neuroblastoma cells was determined *in vitro*. ADCC with anti-CD105 mAb TRC105 and aNK cells against MSCs, monocytes, and endothelial cells, which express CD105, was evaluated. Anti-neuroblastoma activity in immunodeficient NSG mice of dinutuximab with aNK cells without or with anti-CD105 mAbs was determined using neuroblastoma cell lines and a patient-derived xenograft.

**Results:** ADCC mediated by dinutuximab with aNK cells against neuroblastoma cells *in vitro* was suppressed by addi-

tion of MSCs and monocytes, and dinutuximab with aNK cells was less effective against neuroblastomas formed with co-injected MSCs and monocytes in NSG mice than against those formed by tumor cells alone. Anti-CD105 antibody TRC105 with aNK cells mediated ADCC against MSCs, monocytes, and endothelial cells. Neuroblastomas formed in NSG mice by two neuroblastoma cell lines or a patient-derived xenograft co-injected with MSCs and monocytes were most effectively treated with dinutuximab and aNK cells when anti-human (TRC105) and anti-mouse (M1043) CD105 antibodies were added, which depleted human MSCs and murine endothelial cells and macrophages from the TME.

**Conclusions:** Immunotherapy of neuroblastoma with anti-GD2 antibody dinutuximab and aNK cells is suppressed by CD105<sup>+</sup> cells in the TME, but suppression is overcome by adding anti-CD105 antibodies to eliminate CD105<sup>+</sup> cells.

## Introduction

Treatment of patients with high-risk neuroblastoma includes myeloablative therapy followed by mAb immunotherapy that targets residual tumor cells expressing disialoganglioside GD2 (1). Nearly all neuroblastomas express GD2 (2), and standard-of-care treatment including chimeric anti-GD2 mAb dinutuximab/ch14.18 has significantly improved event-free and overall survival of patients (1). However, 40% of patients relapse during or after this therapy, and most succumb (1). Mechanisms of treatment failure have not been elucidated.

The tumor microenvironment (TME) can promote tumor development, metastasis, and resistance to chemotherapy and immunotherapy (3–7). Therefore, targeting of specific cells in the TME is a potential therapeutic strategy (8), and the simultaneous targeting of both tumor and TME cells using specific mAbs combined with adoptively transferred effector cells represents a new combinatorial strategy for cancer therapy.

Mesenchymal stromal cells (MSC), tumor-associated macrophages (TAM), and endothelial cells are components of the TME. MSCs have strong immunosuppressive and protumorigenic properties (4, 5, 9, 10). TAMs, which differentiate from monocytes, can promote resistance of tumors to chemotherapy and radiotherapy as well as inhibit T and NK cell function (3). A high frequency of TAMs is associated with a worse prognosis in lung, breast, prostate, thyroid, hepatocellular carcinoma, and follicular lymphoma (10, 11). We have shown experimentally that TAMs stimulate neuroblastoma cell growth *in vitro* and *in vivo* (12) and have demonstrated that high-risk, MYCN-nonamplified neuroblastomas from patients express high levels of TAM-associated genes (CD14, CD16, IL6, and IL6R), which correlated with a poor 5-year event-free survival (13). Therefore, experimental modeling of the TME can appropriately include MSCs and monocyte-derived TAMs.

CD105 (endoglin), a transmembrane coreceptor for both TGFβ and bone morphogenetic protein-9 (BMP-9), is expressed by MSCs, cancer-associated fibroblasts (CAF), proliferating

<sup>1</sup>Children's Hospital Los Angeles and the Saban Research Institute, Los Angeles, California. <sup>2</sup>Department of Pediatrics, Keck School of Medicine, University of Southern California, Los Angeles, California. <sup>3</sup>Department of Pathology and Laboratory Medicine, Keck School of Medicine, University of Southern California, Los Angeles, California. <sup>4</sup>TRACON Pharmaceuticals, Inc., San Diego, California.

**Note:** Supplementary data for this article are available at Clinical Cancer Research Online (<http://clincancerres.aacrjournals.org/>).

**Corresponding Author:** Robert C. Seeger, Children's Hospital Los Angeles, 4650 Sunset Boulevard, MS #57, Los Angeles, CA 90027. Phone 323-361-5618; Fax 323-361-4902; E-mail rseeger@chla.usc.edu

Clin Cancer Res 2019;25:4761–74

doi: 10.1158/1078-0432.CCR-18-3358

©2019 American Association for Cancer Research.

### Translational Relevance

We hypothesized that the tumor microenvironment (TME) can impair the efficacy of antibody therapy of cancer. To test this hypothesis, we determined whether treatment of human neuroblastoma, which expresses disialoganglioside (GD2), with the anti-GD2 antibody dinutuximab, was improved by concomitantly targeting and eliminating CD105<sup>+</sup> cells in the TME. CD105<sup>+</sup> cells, including mesenchymal stromal cells, endothelial cells, and monocytes/macrophages, were killed *in vitro* by anti-CD105 antibody TRC105 combined with activated NK cells. These cells also were eliminated from the TME of human neuroblastomas growing in NSG mice by combining TRC105 with dinutuximab and adoptively transferred activated NK cells. These data suggest that treatment of patients with high-risk neuroblastoma with dinutuximab may be enhanced by concurrently reducing MSCs, macrophages, and endothelial cells in the TME with anti-CD105 mAb therapy. They also suggest that antibody therapy of other malignancies may be improved by concurrent elimination of CD105<sup>+</sup> cells in the TME.

angiogenic endothelial cells, and monocytes/macrophages in tumors including neuroblastomas (6, 14–18). Thus, CD105 is a potentially important target for immunotherapeutic elimination of cells of the TME. The anti-CD105 antibody TRC105 is a chimeric IgG1 antibody that binds human CD105 with high affinity and induces ADCC by Fc-receptor-expressing cells against CD105<sup>+</sup> target cells such as proliferating endothelial cells (14). TRC105 also binds to murine CD105 (19, 20). TRC105 has been tested in phase I and II clinical trials for patients with prostate, ovarian, bladder, breast, hepatocellular, and urothelial cancer with minimal side effects (21–23) and is currently being studied in a phase III trial in patients with angiosarcoma (NCT02979899).

We show that MSCs derived from the bone marrow of patients with neuroblastoma strongly express CD105 and that these cells are susceptible to ADCC induced by TRC105 and *ex vivo*-activated human NK (aNK) cells. Similarly, endothelial cells and monocytes also express CD105 and are sensitive to ADCC induced by TRC105 and aNK cells. On the basis of these data and those cited above, we hypothesized that depletion of human and mouse cells in the TME using TRC105 and anti-mouse CD105 mAb M1043 combined with adoptively transferred aNK cells would alter the TME and thereby improve the efficacy of dinutuximab combined with aNK cells. Using coinjection of human neuroblastoma cells with human MSCs and monocytes to model the TME, we show that treatment with TRC105 and M1043 depleted human MSCs as well as murine endothelial cells and TAMs from the TME and markedly improved the efficacy of dinutuximab combined with adoptively transferred aNK cells against human neuroblastoma cells growing in immunodeficient NSG mice.

### Materials and Methods

#### Neuroblastoma cells, MSCs, monocytes, HUVECs, aNK cells, and reagents

Human neuroblastoma cell lines CHLA-255, CHLA-136, their firefly luciferase-expressing counterparts CHLA-255-Fluc and

CHLA-136-Fluc, as well as the *Renilla* luciferase-expressing cell line CHLA-136-hRL, were maintained in Iscove's Modified Dulbecco's Medium (IMDM) with 12% FBS (Omega Scientific). CHLA-255-Fluc, CHLA-136-Fluc, and CHLA-136-hRL cells were transduced with the firefly luciferase (Fluc) gene or humanized *Renilla* luciferase (hRL) gene using a lentivirus vector. CHLA-255 cells do not have gene amplification of *MYCN* and do not detectably express the protein (24), but do overexpress c-Myc (S. Asgharzadeh, personal communication). CHLA-136 cells have gene amplification of *MYCN* and express its protein (24, 25). The neuroblastoma patient-derived xenograft (PDX) COG-N-415x expresses mutated ALK (F1174L) and has amplification of *MYCN* [kindly provided by Dr. C. Patrick Reynolds, the Children's Oncology Group (COG) Cell Culture and Xenograft Repository, www.COGcell.org]. Both cell lines and the PDX express cell surface GD2 by flow cytometry (Supplementary Fig. S1). Cells were tested for *Mycoplasma* using MycoAlert (Lonza) and the genetic identity of these cell lines and the PDX was authenticated using Promega PowerPlex 16 HS kits (Promega, catalog no. DC6531).

MSCs were cultured from fresh bone marrow samples from patients with neuroblastoma enrolled in biology studies of the New Approaches to Neuroblastoma Therapy consortium (NANT) or the COG as approved by the Institutional Review Board at Children's Hospital Los Angeles (CHLA, Los Angeles, CA). Briefly,  $1 \times 10^7$  mononuclear cells were isolated from bone marrow by Ficoll-Hypaque (Sigma-Aldrich) density gradient centrifugation, plated in 75-cm<sup>2</sup> flasks, and cultured in Eagle  $\alpha$ -minimum essential medium (Alpha Modification, Sigma-Aldrich) supplemented with 10% FBS and penicillin/streptomycin (Sigma-Aldrich). After 24 hours, cultures were washed twice with PBS to remove nonadherent cells, and adherent cells were maintained with medium replenishment every 3–4 days until approximately 80% confluence was reached 1–2 weeks after initiation. These cells all expressed MSC-associated markers CD44, CD73, CD90, and CD105 and did not express CD31, CD34, CD45, or HLA-DR (15). Cultures were continued in this manner, and after 3–4 passages, MSCs were viably frozen in aliquots. MSCs from four different donors were tested for *in vitro* and *in vivo* experiments with similar results (Supplementary Table S1).

Monocytes were isolated from healthy donor peripheral blood mononuclear cells (PBMC) using EasySep Negative Selection Monocyte Isolation Kits (StemCell Technologies). Purity was 95%–96% as determined by CD14 surface staining measured by flow cytometry. Human umbilical vein endothelial cells (HUVEC) were purchased from AllCells, LLC and maintained in HUVEC Basal Medium containing 10% Stimulatory Supplement from AllCells in 0.1% gelatin precoated flasks. Where indicated, MSCs, monocytes, and HUVECs were transduced with the firefly luciferase gene as described above.

NK cells from healthy donor PBMCs were propagated and activated *ex vivo* using K562-mbIL21 feeder cells and IL2, as described previously (27, 28). T cells were depleted at day 7 of culture using EasySep Magnet-activated Cell Sorting (StemCell Technologies). aNK cells, which were greater than 99% CD56 and CD16 positive by flow cytometry after 14 days of *ex vivo* propagation, were aliquoted and viably frozen in Cryoprotective Medium (Lonza). A list of cells and their donors is presented in Supplementary Table S1.

Anti-GD2 chimeric mAb dinutuximab was provided by the National Cancer Institute at Frederick (Frederick, MD). Anti-human CD105 chimeric IgG1 mAb TRC105 and rat anti-mouse CD105 IgG1 mAb M1043 were provided by TRACON Pharmaceuticals, Inc.

#### *In vitro* cytotoxicity assays

Cryopreserved K562-mbIL21-propagated aNK cells (28) were thawed and cultured in 10% FBS-RPMI1640 with 100 IU/mL IL2 for 48 hours and then used for cytotoxicity assays against neuroblastoma cell lines, MSCs, monocytes, and HUVECs. For the 6-hour assay, CHLA-136-Fluc and CHLA-255-Fluc were labeled with the fluorescent dye calcein-AM (Thermo Fisher Scientific) for 30 minutes at 37°C, washed, and then  $1 \times 10^4$  cells/well were plated in 96-well plates with nonlabeled aNK cells at various effector-to-target (E:T) ratios, without or with dinutuximab and/or TRC105. After 6 hours, retained calcein was quantified using digital imaging microscopy (28). For the 24-hour assay,  $5 \times 10^3$  cells/well of MSC-Fluc, monocyte-Fluc, or HUVEC-Fluc cells were plated with nonlabeled aNK cells at various E:T ratios with or without mAbs TRC105 or dinutuximab. Surviving cells were quantified after 24 hours by adding D-luciferin (150 µg/mL; Biosynth) and measuring bioluminescence intensity with a GloMax-Multi Detection System (Promega).

#### Flow cytometry

Cell surface staining was performed as described previously (26, 28, 29). Antibodies are listed in Supplementary Table S2.

#### IHC staining and quantification

For measurement of mouse CD34<sup>+</sup> endothelial cells and F4/80<sup>+</sup> mouse macrophages in tumors, tissues were fixed in formalin, embedded in paraffin, cut into 5-µm sections, and stained using an automated Leica BOND RX Autostainer (Leica Biosystems). Rabbit anti-mouse CD34 mAb (clone EP373Y, Abcam, 1:4,000 dilution) was used to stain mouse endothelial cells. Tumor microvessel density (MVD) was assessed according to criteria described by Weidner and colleagues (30, 31). Briefly, the entire tumor section was scanned at low magnification ( $\times 100$ ) to find areas of highest tumor vascular density, and images of four such fields were digitally acquired at high magnification ( $\times 200$ ). MVD was quantified by image analysis with ImageJ software (NIH, Bethesda, MD), and an average for eight fields from two sections of each tumor was determined. For assessment of mouse macrophages in tumors, a rat anti-mouse F4/80 mAb (clone CI-A-3, Abcam, 1:800) was used. The tumor area of each section was screened, and four areas with highest density of macrophages were selected and digitally acquired. Pixels of these four areas were quantified using ImageJ software, and an average of eight fields from two sections of each tumor was determined.

For IHC analysis of CD105 expression by human neuroblastoma tumors, paraffin-embedded tumor tissues were obtained from the COG Biorepository by H. Shimada (COG study ANBL00B1). Informed consent was obtained from parents or legal guardians of patients by COG investigators. The study (principal investigator, H. Shimada) was approved by the CHLA Institutional Review Board (CCI11-00261, Neuroblastoma Pathology) and performed under the U.S. Common Rule. IHC was performed on human neuroblastomas that were obtained at

diagnosis from patients with high-risk, clinical stage IV (metastatic) disease and that were MYCN-amplified (MYCN-A) or MYCN-nonamplified (MYCN-NA) with no other known distinguishing clinical factors. These tumors were stained for human CD31,  $\alpha$ SMA, and CD105, which allowed quantification of antigen expression by the endothelial cells of blood vessels and by MSCs/CAFs in tumor stroma. Three sequential immunostainings with Leica Bond RTU primary antibodies were performed on each slide using the Leica Bond Rx IHC platform. Briefly, after epitope retrieval, the first staining was performed with anti-CD31, and after obtaining images, positive signals (Liquid Fast Red, red color) were removed by soaking slides with 1% acid alcohol and acetone. Slides were again subjected to epitope retrieval and then immunostained a second time with anti- $\alpha$ SMA antibody (Liquid Fast Red, red color). After obtaining images, positive signals were removed as above. After epitope retrieval, slides were immunostained for the third time with anti-CD105 antibody. CD105 staining (3, 3'-Diaminobenzidine, brown color) was quantified with Aperio ImageScope software (Leica Biosystems).

#### *In vivo* murine neuroblastoma model and treatment

All animal experiments were performed in accordance with a protocol approved by the Institutional Animal Care and Use Committee of CHLA. In the renal capsule model in NSG mice (32), the left kidney of anesthetized mice was exteriorized and  $1 \times 10^6$  neuroblastoma cells (CHLA-255-Fluc, CHLA-136-Fluc or COG-N-415x PDX cells) were injected under the renal capsule, either alone or mixed with MSCs ( $0.5 \times 10^6$ ) and monocytes ( $0.5 \times 10^6$ ). Subsequently, the kidney was returned to the retroperitoneal space, the muscle was closed with a single 4-0 polysorb suture, and the skin was closed with a skin clip. Groups of mice were age and sex-matched. Tumor growth in mice injected with luciferase-expressing cell lines was assessed by bioluminescence imaging using a Xenogen IVIS 100 instrument (IVIS Lumina XR System, Caliper Life Sciences). Treatment with aNK cells plus mAbs intravenously began on day 3 or 4 after neuroblastoma cell injection. Treatments were administered twice a week for four weeks with aNK cells ( $10^7$ /mouse, immediately after thawing), dinutuximab (15 µg/mouse), TRC105 (100 µg/mouse), or mAb M1043 (100 µg/mouse) alone or in different combinations as indicated. Recombinant human IL2 (2 µg/mouse) and IL15 (5.0 µg/mouse) were injected intravenously with aNK cells.

#### Statistical analysis

Data were analyzed using Stata statistical software (version 11.2) and are represented as mean  $\pm$  SE unless otherwise stated. Student *t* test was performed to compare two groups. ANOVA was utilized for multiple comparisons. Analysis of tumor bioluminescence data was performed by transforming the photon flux for each mouse using the log (flux + 1) transformation and then area under the growth curve (AUC) was calculated and used in the analysis to compare differences between treatment groups. Mouse survival time was defined as the length of time (in days) from tumor cell injection until the end of the study or time of euthanasia due to disease progression that caused symptoms (e.g., > 15% weight loss, weakness, seizures, inability to obtain food or water, inability to stand, and/or paralysis). The Kaplan-Meier analysis was used to generate survival curves. A *P* value of < 0.05 was considered statistically significant.

Wu et al.

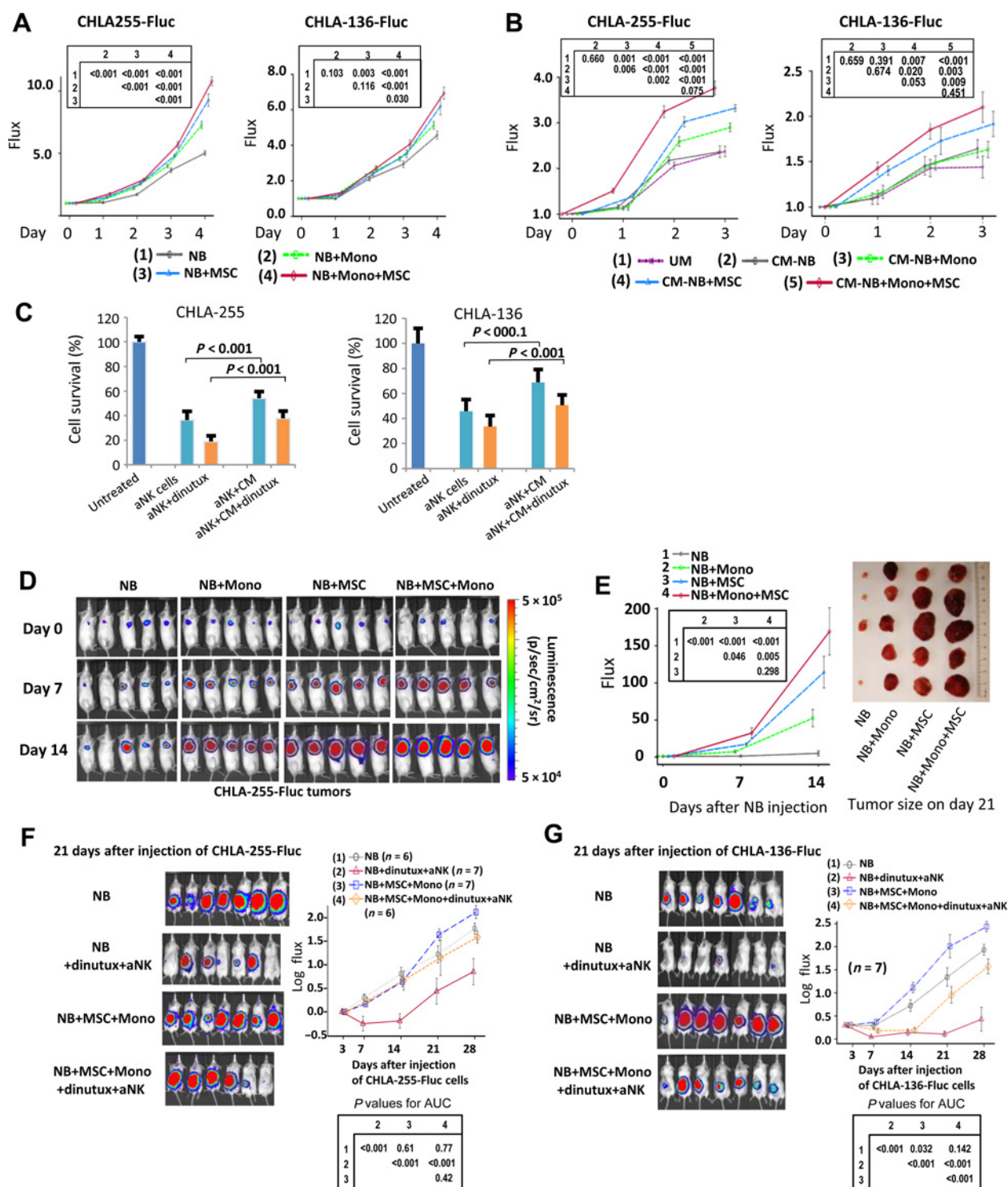


**Figure 1.**

Human MSCs and monocytes enhance neuroblastoma (NB) cell growth and impair antineuroblastoma activity of aNK cells plus anti-GD2 mAb dinutuximab. **A**, Effects of coculture of human MSCs and monocytes with neuroblastoma cell lines on the propagation of neuroblastoma cell lines *in vitro*. CHLA-255-Fluc ( $5 \times 10^5$ ) or CHLA-136-Fluc ( $5 \times 10^5$ ) cells were cultured alone or with MSCs ( $1 \times 10^5$  from bone marrow of patients with neuroblastoma), monocytes ( $5 \times 10^3$ , freshly isolated from PBMCs of healthy donors), or MSCs + monocytes in a 96-well microplate in 200  $\mu$ L of culture medium per well. (Continued on the following page.)

## Results

### Human MSCs and monocytes enhance neuroblastoma cell growth and impair ADCC mediated by dinutuximab with aNK cells *in vitro* and *in vivo*

We hypothesized that cross-talk between MSCs, macrophages, and neuroblastoma cells in the TME could enhance neuroblastoma cell growth and suppress ADCC mediated by aNK cells with dinutuximab. Human neuroblastoma cell lines CHLA-255-Fluc or CHLA-136-Fluc were cocultured without or with MSCs from patients with neuroblastoma and without or with purified human monocytes for 96 hours. Addition of MSCs increased neuroblastoma cell numbers as measured by bioluminescence, and adding monocytes further increased tumor cell numbers (Fig. 1A). We then tested whether conditioned medium (CM) from tri-cell cocultures of neuroblastoma cells, MSCs, and monocytes also would promote tumor cell growth and whether it would suppress aNK cell direct cytotoxicity and ADCC. The growth of CHLA-255-Fluc and CHLA-136-Fluc was significantly increased after 72 hours of culture with 50% CM collected from coculture of CHLA-255 cells, MSCs, and monocytes (Fig. 1B). Both direct cytotoxicity and ADCC of aNK cells with dinutuximab against CHLA-255 and CHLA-136 cells were significantly suppressed by the presence of 50% CM from the tri-cell cocultures (Fig. 1C).

Analysis of CMs of neuroblastoma cell lines cultured alone, with MSCs or monocytes, or with both MSCs and monocytes showed IL6, IL8, IL10, G-CSF, GRO (CXCL1), MDC (CCL22), IP-10 (CXCL10), RANTES (CCR5), and TGF $\beta$ 1 to be increased in cocultures compared with NB cells alone (Supplementary Figs. S2–S25). TGF $\beta$ 1 was released by neuroblastoma cell lines and further increased by their coculture with monocytes as reported previously (29). Compared with neuroblastoma cells alone, TGF $\beta$ 1 also was increased in CMs of cocultures of neuroblastoma cells and MSCs. TGF $\beta$ 1 was increased the greatest in CMs of neuroblastoma cells cocultured with both monocytes and MSCs (Supplementary Fig. S5). Together, these data suggest that neuroblastoma cells interacting with MSCs and monocyte-derived cells can produce an environment that includes multiple cytokines including TGF $\beta$ 1 that could promote tumor growth and suppress NK-cell cytotoxicity.

Next, we used an immunodeficient mouse model to determine whether MSCs and monocytes could promote human neuroblastoma cell growth *in vivo*. CHLA-255-Fluc cells were injected

subcutaneously in the area of the right shoulder of NSG mice either alone, with MSCs or monocytes, or with both MSCs and monocytes. Both MSCs and monocytes promoted tumor growth significantly, and the combination of all three cell types stimulated the greatest growth (Fig. 1D and E).

We also determined whether the antitumor efficacy of dinutuximab with aNK cells *in vivo* was suppressed by coinjecting MSCs and monocytes with neuroblastoma cells. CHLA-255-Fluc cells ( $1 \times 10^6$ ) alone, or with MSCs ( $0.5 \times 10^6$ ) plus monocytes ( $0.5 \times 10^6$ ) were injected into NSG mice under the capsule of the left kidney (32), and concomitant treatment with aNK cells ( $1 \times 10^7$ /mouse, *i.v.*) and dinutuximab (15  $\mu$ g/mouse, *i.v.*) was started on day 3 and continued twice a week for 4 weeks. IL2 (2  $\mu$ g/mouse) and IL15 (5  $\mu$ g/mouse) were injected intravenously along with aNK cells and dinutuximab. This models treatment of minimal disease. Tumor response was assessed weekly by bioluminescence imaging. Fig. 1F shows that tumors formed by coinjection of MSCs and monocytes were significantly less sensitive to dinutuximab plus aNK cells than tumors formed by CHLA-255-Fluc cells alone. Similarly, treatment with aNK cells plus dinutuximab was less effective against tumors formed by coinjection of CHLA-136-Fluc cells, MSCs, and monocytes than against those formed by CHLA-136-Fluc cells alone (Fig. 1G).

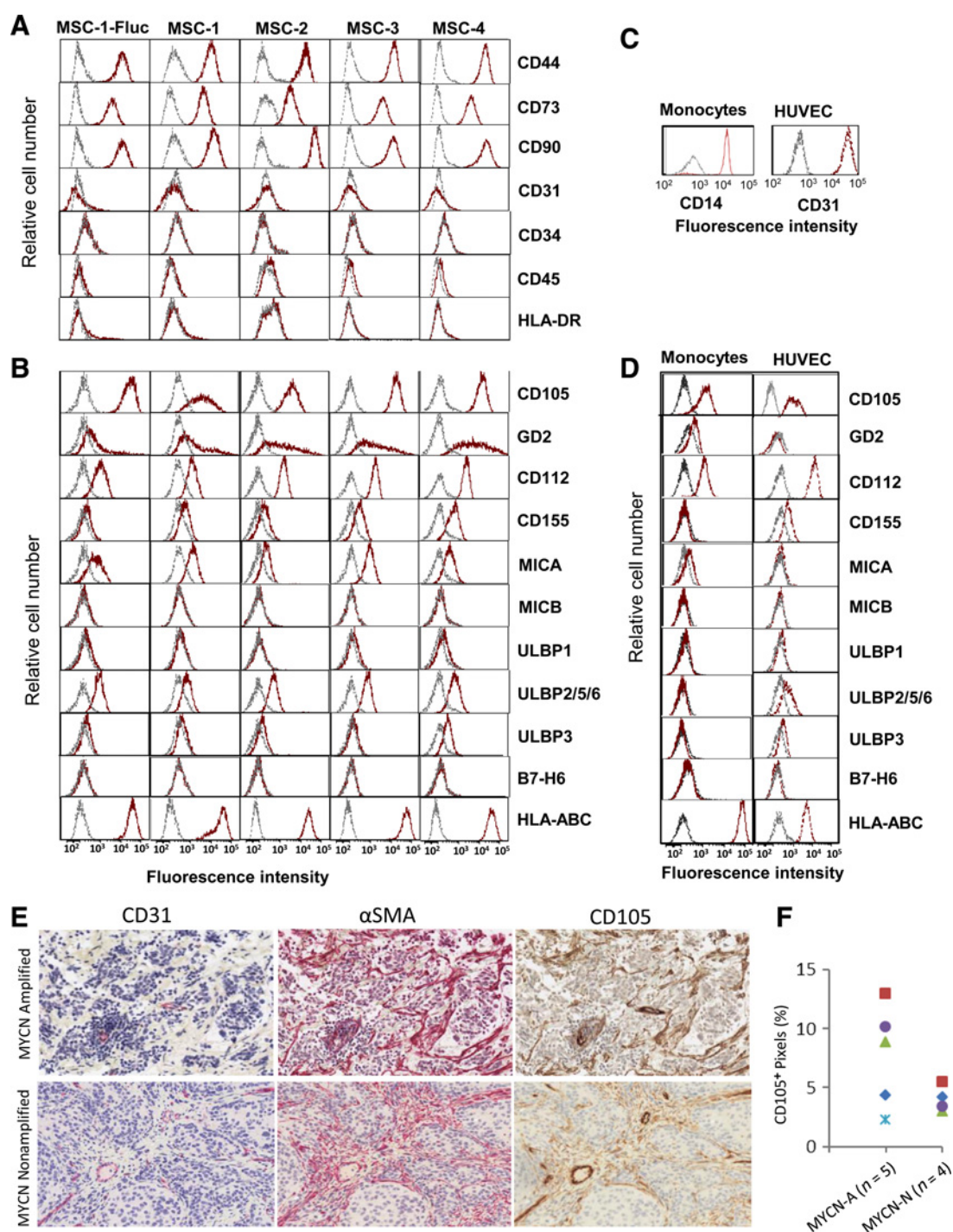
### CD105 is expressed by cultured human MSCs, monocytes, and endothelial cells and by endothelial and stromal cells in human neuroblastoma tumors

We determined whether human MSCs could be targeted with anti-CD105 mAb for immunotherapeutic elimination. MSCs (CD44<sup>+</sup>CD73<sup>+</sup>CD90<sup>+</sup>CD31<sup>-</sup>CD34<sup>-</sup>CD45<sup>-</sup>HLA-DR<sup>-</sup>) were cultured from bone marrows of 4 patients with high-risk neuroblastoma (Fig. 2A). Importantly, the MSCs expressed CD105, GD2, and ligands for NK-cell cytotoxicity receptors DNAM-1 (CD112 and CD155) and NKG2D (MICA and ULBP2/5/6; Fig. 2B). CD105 was expressed by all MSCs, and GD2 was expressed by approximately half of the MSCs from each patient.

Monocytes (Fig. 2C) also expressed CD105, which was consistent with a previous report (18), and also expressed CD112, a ligand for DNAM-1 (Fig. 2D). Endothelial cells are known to express CD31 and CD105, and, as expected, HUVECs expressed these antigens but not GD2 (Fig. 2C and D). HUVECs also

(Continued.) Propagation of NB cells was determined by luminescence intensity using a Promega plate reader after 1, 2, 3, and 4 days of coculture, which was before cell overgrowth occurred. Each condition was examined in eight replicate wells. Area under the curve (AUC) was calculated using baseline corrected flux values and plotted as mean  $\pm$  SE; linear regression was used to examine differences. Analysis was performed with Stata 11. *P* values refer to two-sided tests and are shown in the inserted boxes. **B**, Effects of conditioned medium (CM) collected from cultures of CHLA-255-Fluc cells alone or from cocultures of CHLA-255-Fluc cells with MSCs, monocytes, or MSCs + monocytes, on the growth of neuroblastoma cell lines *in vitro*. CMs were collected from coculture of CHLA-255-Fluc ( $1 \times 10^6$ ), monocytes ( $1 \times 10^6$ ), and MSCs ( $0.25 \times 10^6$ ) for 72 hours in 3 mL of medium. Fifty-percent CMs, or fresh unconditioned medium (UM) as a control, were added to cultures of CHLA-255-Fluc ( $2 \times 10^5$ ) or CHLA-136-Fluc ( $2 \times 10^5$ ) cells (200  $\mu$ L total volume) in a 96-well plate. Propagation of neuroblastoma cells was determined for eight replicates by luminescence intensity, as above. **C**, Effect of CM from coculture of CHLA-255-Fluc cells, MSCs, and monocytes on cytotoxicity of aNK cells  $\pm$  dinutuximab (dinutux) against neuroblastoma cell lines. aNK cells were cultured ( $1 \times 10^4$  cells/0.1 mL/well) for 24 hours with added CM (50% V/V), then direct cytotoxicity and ADCC (E:T ratio = 1:1) with dinutuximab (0.1  $\mu$ g/mL) against CHLA-255-Fluc or CHLA-136-Fluc cells were quantified using the calcein-AM assay (mean  $\pm$  SD of eight replicate cultures per condition) after a 6-hour coculture. Paired *t* test. **D** and **E**, Effect of coinjecting human monocytes ( $2 \times 10^6$ ), MSCs ( $1 \times 10^6$ ), or both with CHLA-255-Fluc cells ( $4 \times 10^6$ ) on subcutaneous tumor growth in NSG mice. Tumor growth was quantified by bioluminescent imaging and by tumor size at time of sacrifice. **F** and **G**, Effect of coinjection of neuroblastoma cells with MSCs and monocytes under the left kidney capsule of NSG mice on neuroblastoma growth and on sensitivity to adoptively transferred aNK cells plus dinutuximab. CHLA-255-Fluc ( $1 \times 10^6$ ) or CHLA-136-Fluc ( $1 \times 10^6$ ) cells were either injected alone or coinjected with MSCs ( $0.5 \times 10^6$ ) and monocytes ( $0.5 \times 10^6$ ). Treated mice received aNK cells ( $1 \times 10^7$ /mouse, *i.v.*) and dinutuximab (15  $\mu$ g/mouse, *i.v.*) starting on day 3 and continuing twice a week for four weeks. Tumor growth was monitored by bioluminescence imaging, and images obtained 21 days after neuroblastoma cell injection are shown. Total flux of tumors in untreated and treated mice was adjusted to baseline pretreatment values, log<sub>10</sub> transformed, and plotted as mean  $\pm$  SE, and significance of differences between AUCs was determined by linear regression analysis.

Wu et al.

**Figure 2.**

Expression of CD105, GD2, and ligands for natural cytotoxicity receptors on human MSCs, monocytes, and HUVECs, and expression of CD105 in human neuroblastoma (NB) tumors. **A**, MSCs were cultured from bone marrow of four patients with neuroblastoma (passage 4–6), and their identity was confirmed by analysis of CD44, CD73, CD90, CD31, CD34, CD45, and HLA-DR using flow cytometry. **B**, MSCs were characterized for expression of potential target molecules, including CD105, GD2, and ligands for natural cytotoxicity receptors DNAM-1 (CD112 and CD155), NKG2D (MICA, MICB, ULBP1, ULBP2/5/6, and ULBP3), and NKp30 (B7-H6), and for HLA-ABC. **C**, Monocytes were identified by expression of CD14, and HUVECs by CD31. **D**, Monocytes and HUVECs were analyzed for expression of CD105, GD2, and ligands for natural cytotoxicity receptors. **E**, Representative IHC stains for CD105, CD31, and  $\alpha$ SMA in high-risk human neuroblastoma tumors with or without *MYCN* amplification. **F**, Expression of CD105 in high-risk *MYCN*-amplified ( $n = 5$ ) and nonamplified ( $n = 4$ ) human NBs. Primary tumors were obtained from patients with metastatic disease but without other known distinguishing clinical factors. Aperio ImageScope software was used for quantification of CD105 expression on ECs (CD105<sup>+</sup>CD31<sup>+</sup>) and pericytes (CD105<sup>+</sup> $\alpha$ SMA<sup>+</sup>) in vasculature and on spindle-shaped MSCs/CAFs (CD105<sup>+</sup> $\alpha$ SMA<sup>+</sup>) in stroma.

expressed DNAM-1 ligands (CD112 and CD155) and the NKG2D ligand(s) ULBP2/5/6 (Fig. 2D).

The clinical relevance of targeting CD105<sup>+</sup> cells in the TME was supported by the presence of spindle-shaped CD31<sup>-</sup>αSMA<sup>+</sup>CD105<sup>+</sup> nonvascular stromal MSCs/CAFs in primary, clinical stage IV, high-risk, MYCN-amplified and nonamplified neuroblastomas using IHC (Fig. 2E). Importantly, IHC also demonstrated vascular-associated CD31<sup>+</sup>αSMA<sup>-</sup>CD105<sup>+</sup> endothelial cells and CD31<sup>-</sup>αSMA<sup>+</sup>CD105<sup>+</sup> pericytes. Evaluation of five MYCN-amplified and four MYCN-nonamplified tumors demonstrated that all contain these cells expressing CD105 (Fig. 2F). Together, these experimental and clinicopathologic data, along with our previous demonstration of CD163<sup>+</sup> macrophages in primary human neuroblastomas (13), supports strategies aimed at elimination of immunosuppressive cells from the TME by utilizing aNK cell direct cytotoxicity and ADCC mediated by anti-CD105 mAb.

**CD105 is a target on MSCs, monocytes, and endothelial cells for ADCC mediated by anti-CD105 antibody TRC105 with aNK cells, and anti-CD105 mAbs improve treatment of neuroblastomas with dinutuximab and adoptively transferred aNK cells in NSG mice**

Next, we evaluated aNK cell-mediated direct cytotoxicity and ADCC with anti-CD105 mAb TRC105 and with anti-GD2 mAb dinutuximab against human MSCs, monocytes, and HUVECs. aNK cells alone were cytotoxic for these cells after 24 hours of coculture, and adding TRC105 significantly increased cytotoxicity, especially against MSCs (Fig. 3A). In contrast, TRC105 without aNK cells had no effect on MSC, monocyte, or HUVEC survival. Dinutuximab also increased aNK-cell cytotoxicity against MSCs but not against GD2-negative monocytes or HUVECs (Fig. 3A). These *in vitro* experiments with aNK cells confirm that TRC105 can induce ADCC against endothelial cells and for the first time show that TRC105 can induce ADCC against MSCs and monocytes.

We also determined whether NB cell lines express CD105 and, if so, whether they can be targeted with TRC105 for ADCC. Only CHLA-255-Fluc cells among nine neuroblastoma cell lines appreciably expressed CD105 (Supplementary Fig. S6A). aNK cells mediated ADCC with TRC105 against CHLA-255-Fluc cells but not against two other tested neuroblastoma cell lines (Supplementary Fig. S6B and S6C).

To extensively evaluate whether targeting CD105<sup>+</sup> cells in the TME can enhance the anti-neuroblastoma effect of dinutuximab with aNK cells *in vivo*, we used the CHLA-136-Fluc or CHLA-255-Fluc neuroblastoma cell lines or COG-N-415x PDX cells for the tri-cell (NB:MSC:monocyte) subrenal capsule model in NSG mice. Because mouse MSCs, monocytes, and endothelial cells might become involved in tumor development and because TRC105 binds with low affinity to mouse CD105, we hypothesized that addition of rat anti-mouse CD105 mAb M1043 would further improve the treatment. Mice injected with CHLA-136-Fluc cells ( $1 \times 10^6$ ), MSCs ( $0.5 \times 10^6$ ), and monocytes ( $0.5 \times 10^6$ ) received aNK cells, dinutuximab, and TRC105 plus M1043, alone or in different combinations for four weeks (twice a week) beginning 4 days after tumor cell injection (Fig. 3B–E). Neither aNK cells alone nor anti-CD105 mAbs (TRC105 plus M1043) alone suppressed growth of tumors. Decreased tumor growth and prolonged survival was induced by dinutuximab alone, by the three mAbs combined without aNK cells, and by dinutuximab

plus aNK cells. However, the greatest efficacy in both decreasing tumor growth and prolonging mouse survival was obtained by addition of TRC105 and M1043 to dinutuximab plus aNK cells (Fig. 3B–E).

To confirm these findings, CHLA-255-Fluc cells or COG-N-415x PDX cells were coinjected under the renal capsule with MSCs and monocytes (Fig. 4). Treatment of mice bearing CHLA-255-Fluc tumors with TRC105 plus M1043, or the combination of TRC105, M1043, and aNK cells suppressed tumor growth but did not prolong survival. Treatment with dinutuximab alone, or dinutuximab plus aNK cells, significantly decreased tumor growth and prolonged survival (Fig. 4A–C). The combination of dinutuximab, TRC105, and M1043 had greater efficacy in suppressing tumor growth and in prolonging survival. However, addition of aNK cells to the combination of dinutuximab, TRC105, and M1043 resulted in the largest decrease in tumor growth and longest prolongation of survival (Fig. 4A–C). For mice bearing COG-N-415x tumors, survival was not increased by treatment with the combination of TRC105, M1043, and aNK cells. However, mice treated with dinutuximab plus aNK cells had increased survival, and those treated with dinutuximab, TRC105, M1043, and aNK cells had the longest survival (Fig. 4D).

We also tested whether adding TRC105 or M1043 individually would improve the efficacy of dinutuximab with aNK cells. TRC105 improved growth suppression and survival when added to dinutuximab and aNK cells. Addition of only M1043 to dinutuximab with aNK cells improved suppression of tumor growth in the first 21 days compared with dinutuximab alone with aNK cells. However, this early suppression of growth by addition of M1043 did not persist at days 28 and 35, and survival was not improved (Supplementary Fig. S7A–S7C). Together, these findings support the conclusion that ADCC of aNK cells with dinutuximab is most effectively enhanced by TRC105 targeting of CD105<sup>+</sup> cells in the TME.

**Anti-CD105 mAbs and dinutuximab with aNK cells deplete MSCs from the tumor microenvironment, decrease tumor growth, and increase survival**

To simultaneously evaluate the responses of neuroblastoma cells and MSCs to combined treatment with TRC105, M1043, dinutuximab, and aNK cells, CHLA-136-hRL, MSC-Fluc, and monocytes were coinjected under the kidney capsule of NSG mice (Fig. 5). Treatment began on day 4 and continued for four weeks with the same doses and schedule as in Figs. 3 and 4. The responses of MSC-Fluc and CHLA-136-hRL cells to treatment were monitored by bioluminescence imaging weekly on successive days to distinguish signals from the two forms of luciferase. aNK cells combined with neither dinutuximab nor anti-CD105 mAbs significantly decreased the MSC-Fluc signal compared with untreated controls, but flux was significantly decreased by combining aNK cells with both anti-CD105 mAbs and dinutuximab (Fig. 5A and B). Dinutuximab plus aNK cells decreased tumor growth but did not achieve significant prolongation of survival ( $P = 0.11$ ). However, addition of anti-CD105 mAbs to this regimen resulted in significant suppression of tumor growth and prolongation of survival (Fig. 5C and D). aNK cells plus anti-CD105 mAbs had no effect on tumor growth, which correlated with a lack of reduction of MSC-Fluc cells in this group compared with those in untreated control mice. Overall, these data support the importance of simultaneously targeting both CD105<sup>+</sup> MSCs in the TME and GD2<sup>+</sup> tumor cells.

Wu et al.

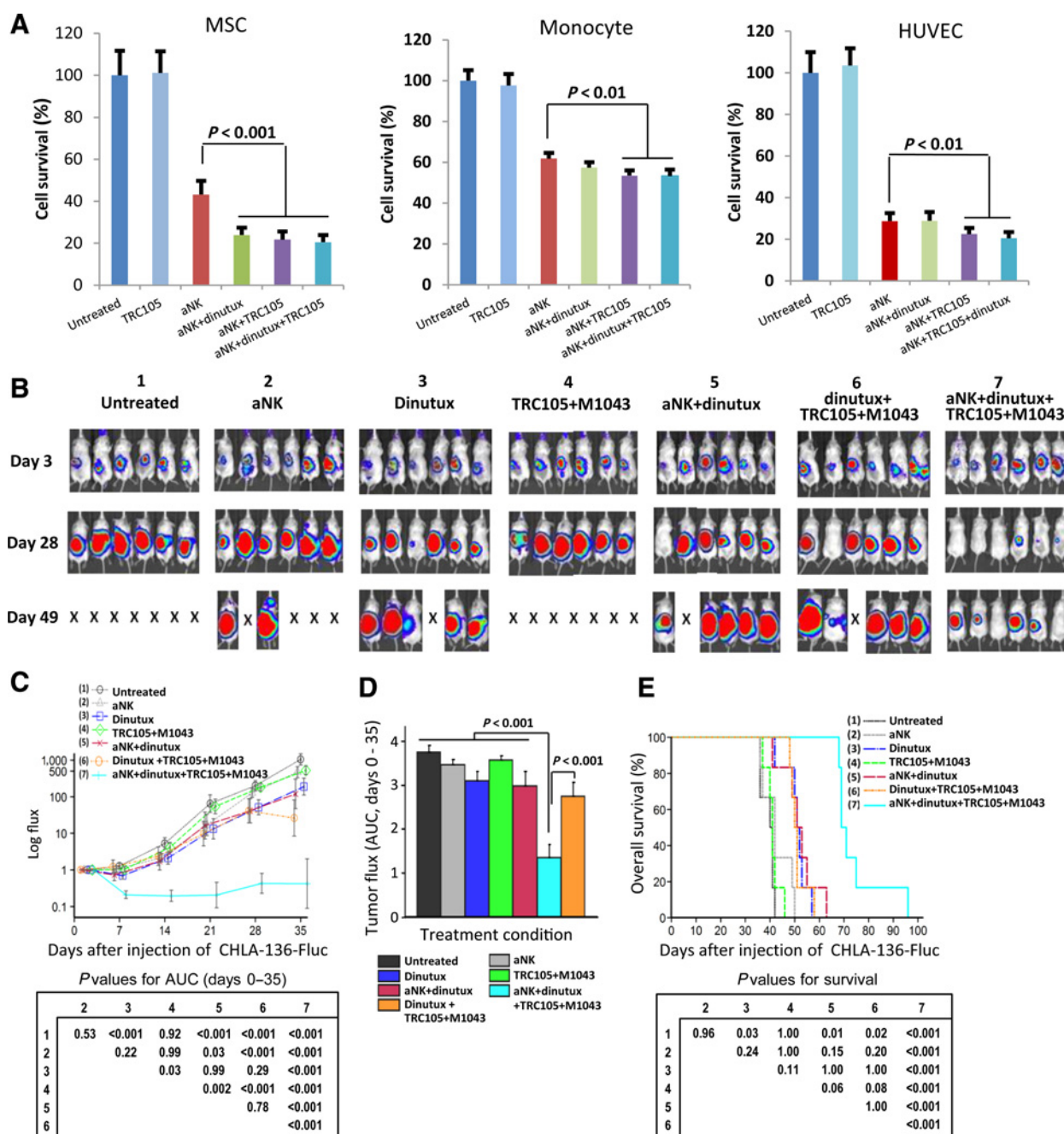


**Figure 3.** Targeting of CD105<sup>+</sup> MSCs, monocytes, and ECs with anti-CD105 mAbs and aNK cells, and growth of CHLA-136-Fluc cells in NSG mice after treatment with dinutuximab and adoptively transferred aNK cells without or with anti-human CD105 mAb TRC105 and anti-mouse CD105 mAb M1043. **A**, aNK cell-mediated direct cytotoxicity and ADCC against MSC-Fluc, monocyte-Fluc, or HUVEC-Fluc cells *in vitro*. aNK cells were cultured with target cells ( $5 \times 10^3$  cells/well) at a 2:1 E:T ratio with or without mAb TRC105 (250 ng/mL) and/or dinutuximab (250 ng/mL) for 24 hours. Surviving target cells were quantified by adding  $\beta$ -luciferin and measuring bioluminescence intensity (mean  $\pm$  SD of eight replicate cultures per condition). **B**, Images of neuroblastoma tumor growth on days 3, 28, and 49 after tumor cell injection. CHLA-136 neuroblastoma cells ( $1 \times 10^6$ ), MSCs ( $0.5 \times 10^5$ ), and monocytes ( $0.5 \times 10^6$ ) were coinjected under the capsule of left kidney of NSG mice, and indicated treatments were administered intravenously twice a week for 4 weeks, starting on day 3. Tumor growth was quantified weekly by bioluminescent imaging. **C**, Total flux of tumors in untreated and treated mice was adjusted to baseline pretreatment values,  $\log_{10}$  transformed, and plotted as mean  $\pm$  SE, and differences were calculated from AUCs. **D**, Bar plot of AUCs from day 0 to day 35 after tumor cell injection. **E**, Kaplan-Meier survival plot for the groups of mice shown in **B** and **C**.

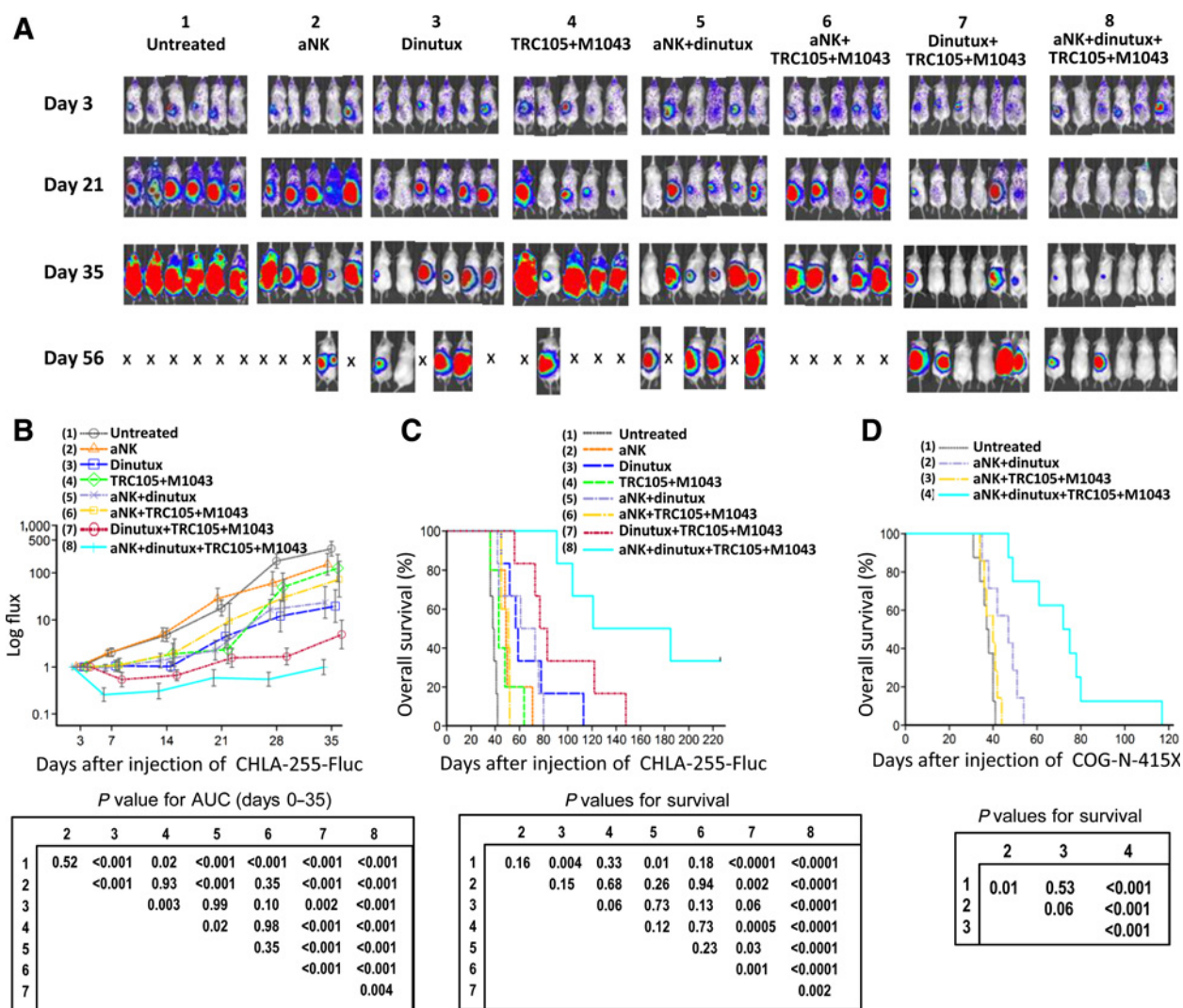


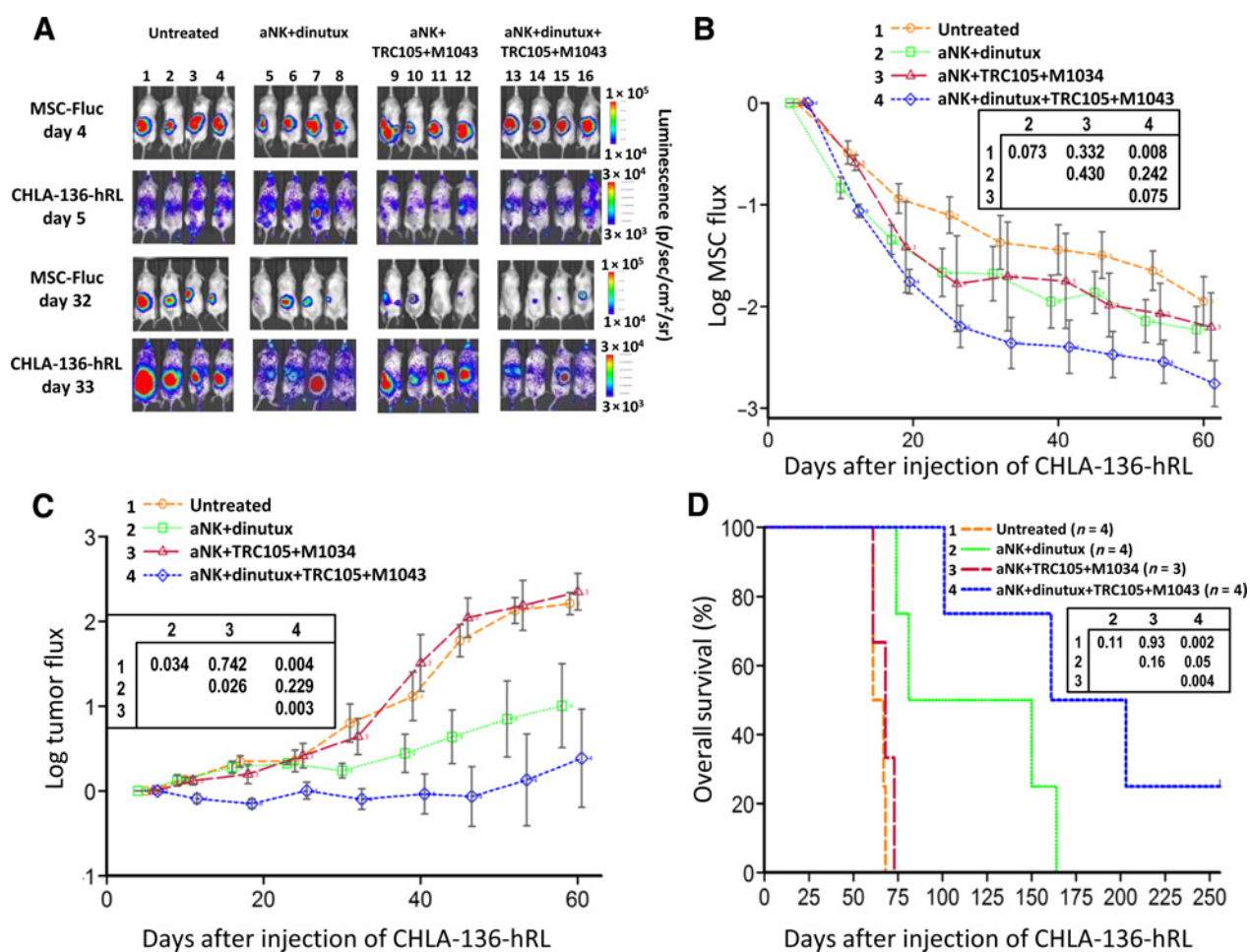
**Figure 4.** Effect of anti-CD105 mAbs and dinutuximab with adoptively transferred aNK cells against CHLA-255-Fluc or COG-N-415x tumors formed with coinjected MSCs and monocytes under the renal capsule of NSG mice. Experimental details are provided in Materials and Methods and Fig. 3. **A**, Images of CHLA-255-Fluc neuroblastoma growth on days 3, 21, 35, and 56 after tumor cell injection. **B**, Total flux of tumors in untreated and treated mice was adjusted to baseline pretreatment values, log<sub>10</sub> transformed, and plotted as mean ± SE, and differences were calculated from AUCs. Therapeutic schedule was as in Fig. 3B. **C**, Kaplan–Meier survival plot for mice injected with CHLA-255-Fluc cells, MSCs, and monocytes and treated as in **A** and **B**. **D**, Kaplan–Meier survival plot for mice injected with PDX COG-N-415x cells, MSCs, and monocytes and treated with aNK cells ± dinutuximab ± anti-CD105 mAbs. Therapeutic schedule was as in Fig. 3B.

**Anti-CD105 mAbs with dinutuximab and aNK cells decrease tumor microvessel density and macrophage infiltration**

To determine whether treatment with aNK cells plus dinutuximab and anti-CD105 mAbs affected microvessels and mouse macrophage infiltration in tumors, microvessel density (MVD) and macrophages were assessed with IHC using anti-mouse CD34 and anti-F4/80 mAbs. MVD and macrophages were quantified using ImageJ software. Tumors from the four groups of mice shown in Fig. 4A (untreated, aNK plus anti-CD105 mAbs, aNK plus dinutuximab, and aNK cells combined with anti-CD105 mAbs and dinutuximab) were stained. Four different areas of the most intense neovascularization or of the highest density of macrophages were analyzed in two different sections of each tumor as detailed in Materials and Methods. MVD was signifi-

cantly decreased by aNK cells plus anti-CD105 mAbs, and was further decreased by combining dinutuximab with aNK cells and anti-CD105 mAbs (Fig. 6A–C). aNK cells + dinutuximab decreased MVD compared with untreated control tumors. However, the mechanism of this decrease is most likely to be indirect due to targeting GD2 expressed by neuroblastoma and mesenchymal stromal cells and so compromising their ability to enhance angiogenesis rather than to direct killing of murine endothelial cells by anti-GD2 dinutuximab + aNK cells. Anti-GD2 IHC of neuroblastoma xenografts demonstrates that mouse endothelial cells do not express GD2, but do express CD34 (Supplementary Fig. S8A). This finding was confirmed by flow cytometry analysis of dissociated CHLA-136-Fluc neuroblastoma tumors from kidneys of NSG mice, which demonstrated that cells

Wu et al.

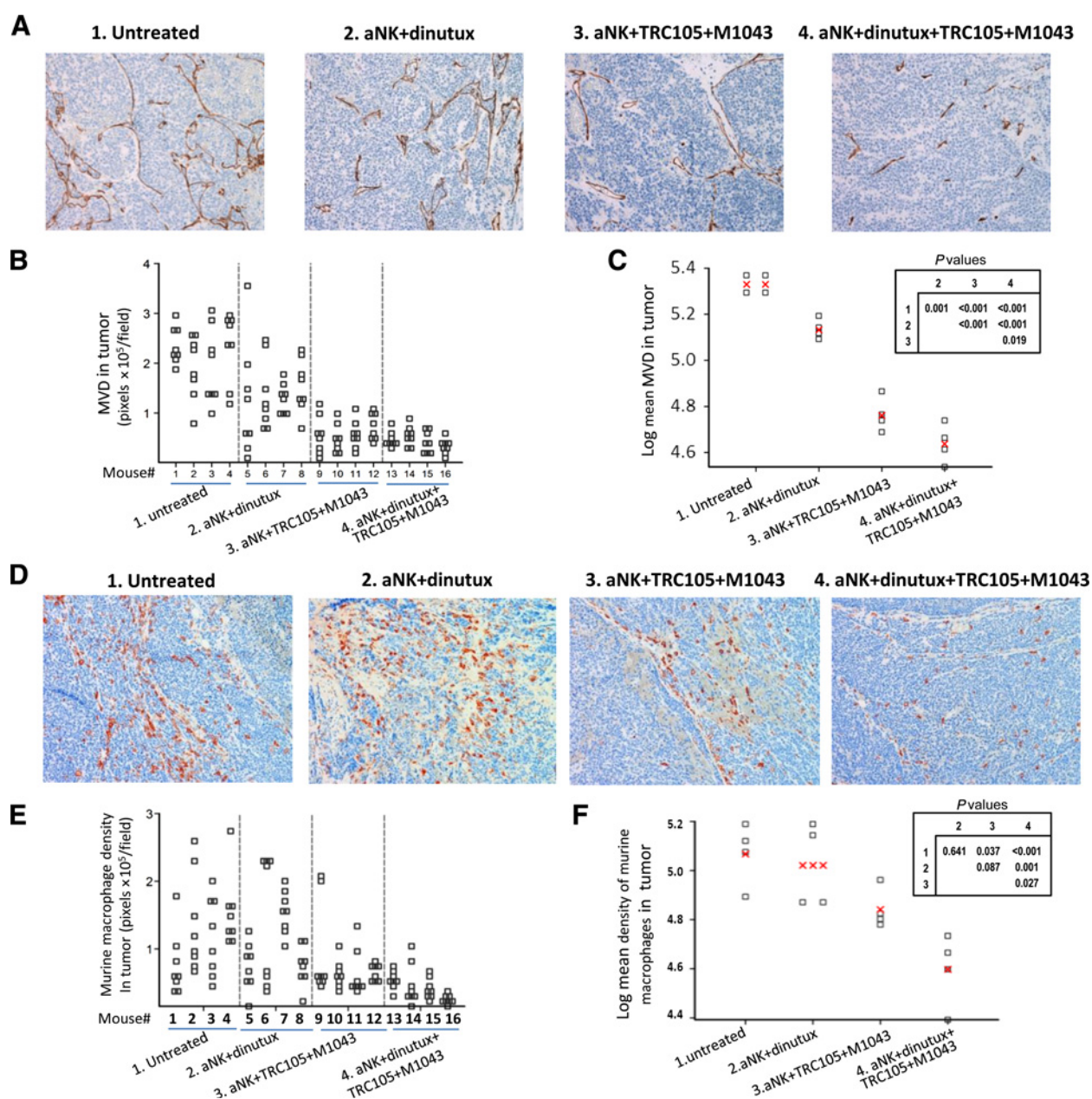
**Figure 5.**

Effect of anti-CD105 and anti-GD2 mAbs with adoptively transferred aNK cells against CHLA-136-hRL neuroblastoma and coinjected MSC-Fluc cells. CHLA-136-hRL ( $1 \times 10^6$ ) cells were coinjected with MSC-Fluc cells ( $0.5 \times 10^6$ ) and monocytes ( $0.5 \times 10^6$ ) under the kidney capsule of NSG mice, and treatments were begun four days later. Neuroblastoma growth and MSC survival were quantified weekly by bioluminescence imaging of flux from humanized *Renilla* luciferase (hRL) and firefly luciferase (Fluc) activity on two consecutive days each week. **A**, Images of NBs on days 5 and 33 and MSCs on days 4 and 32 after injection. **B**, Total flux from MSCs in untreated and treated mice was adjusted to baseline pretreatment values,  $\log_{10}$  transformed, and plotted as mean  $\pm$  SE, and differences between AUCs were calculated. **C**, Total flux from neuroblastoma cells in untreated and treated mice was adjusted to baseline pretreatment values,  $\log_{10}$  transformed, and plotted as mean  $\pm$  SE. Therapeutic schedule was as in Fig. 3B. **D**, Kaplan-Meier survival plot for mice treated as in C.

expressing murine CD31 (a marker of murine endothelial cells) did not express GD2 (Supplementary Fig. S8B). MVD analysis of two complete sections of each tumor provided essentially identical results ( $r = 0.98$ ;  $P < 0.01$ ). The frequency of F4/80<sup>+</sup> cells was significantly decreased by aNK cells plus anti-CD105 mAbs, and was also further decreased by combining dinutuximab with aNK cells and anti-CD105 mAbs (Fig. 6D–F). Depletion of macrophages from neuroblastomas treated with anti-CD105 mAbs plus aNK cells correlated with decreased tumor growth ( $P < 0.001$ , Fig. 4B) but not with mouse survival ( $P = 0.18$ , Fig. 4C), whereas addition of dinutuximab to this treatment resulted in correlation with both decreased tumor growth ( $P < 0.001$ , Fig. 4B) and with increased mouse survival ( $P < 0.0001$ , Fig. 4C). These observations indicate that anti-CD105 mAbs with dinutuximab and aNK cells decrease tumor MVD and macrophage infiltration, which both correlate with efficacy of aNK cell-mediated ADCC.

## Discussion

We demonstrate experimentally that neuroblastoma cells, MSCs, and monocytes together create an environment that suppresses ADCC mediated by aNK cells and promotes tumor growth. *In vitro*, coculture of neuroblastoma cell lines with MSCs and monocytes increased tumor cell numbers. CM from these cocultures suppressed the cytotoxicity of aNK cells alone or with dinutuximab and also promoted tumor cell growth. Notably, these CMs contained multiple cytokines, including TGF $\beta$ 1, which could cause immunosuppression and enhance tumor cell growth (10, 33, 34). Comparison of tumors formed in NSG mice by neuroblastoma cells with coinjected MSCs and monocytes versus those formed by neuroblastoma cells alone demonstrated the former to be less responsive to treatment with dinutuximab and aNK cells, to have increased growth, and to be associated with reduced survival. Because of the

**Figure 6.**

MVD and frequency of murine macrophages in CHLA-255-Fluc tumors treated with anti-CD105 and anti-GD2 mAbs and adoptively transferred aNK cells. Intrarenal tumors from four indicated groups of mice that are shown in Fig. 4 were analyzed. Four mice from each group were sacrificed due to morbidity from tumor growth, at which time they had visually locatable tumors of approximately the same size. Tumors were stained by IHC for murine endothelial cells (CD34) and macrophages (F4/80). **A** and **D** show representative images of CD34<sup>+</sup> microvessels and F4/80<sup>+</sup> macrophages, respectively (200 $\times$  magnification). **B** and **E** show dot plots of MVDs and macrophage frequencies for eight fields (4 fields  $\times$  2 sections) in each tumor from 4 mice per group, which were quantified by digital imaging (ImageJ software). **C** and **F** show the means of tumor MVD and macrophage frequency for each mouse from the four treatment groups. Data were log<sub>10</sub> transformed, and linear regression analysis was used to examine treatment effects on tumor vasculature and macrophages. Red crosses represent group means.

complexity of targeting multiple cytokines and/or their signaling pathways, we determined whether eliminating cells associated with production of these cytokines in the TME, specifically MSC and monocytes/macrophages, would provide a strategy for improving immunotherapy with dinutuximab and aNK cells.

We show that targeted elimination of CD105<sup>+</sup> MSCs, monocytes/macrophages, and endothelial cells from the TME enhances anti-neuroblastoma immunotherapy with dinutuximab and aNK cells. We demonstrate the expression of CD105 on cultured MSCs derived from bone marrow, on monocytes, and on endothelial cells. CD105 was expressed by 90%–100% of

Wu et al.

MSCs from bone marrow of 4 patients with metastatic neuroblastoma. This is consistent with previous studies showing that CD105 is expressed by MSCs and cancer-associated fibroblasts in tumors including neuroblastoma (6, 15, 16). We also find that 40%–90% of MSCs express GD2, which is consistent with previous reports (35, 36). Murine endothelial cells, as well as cultured human monocytes and HUVECs, the latter being a surrogate for tumor endothelial cells, expressed CD105 but not GD2. Ligands for aNK cell cytotoxicity receptors DNAM-1 (CD112 and CD155) and NKG2D (MICA and ULBP2/5/6) are expressed by MSCs, but only the DNAM-1 ligand CD112 is expressed by monocytes and HUVECs. The clinical relevance of CD105 expression by these cell types is supported by our finding that high-risk human primary neuroblastomas, both MYCN gene amplified and nonamplified, contain CD105<sup>+</sup> vascular and stromal cells. These data suggested that anti-CD105 and anti-GD2 mAbs combined with aNK cells could deplete MSCs, monocytes/macrophages, and endothelial cells in the TME and so possibly improve anti-GD2 mAb therapy.

Next, we evaluated aNK cell-mediated direct cytotoxicity and ADCC against MSCs, monocytes, and HUVECs *in vitro*. We show that aNK cells can kill MSCs directly and that even greater killing results from ADCC with anti-CD105 mAb TRC105 and anti-GD2 mAb dinutuximab. In addition, monocytes and HUVECs can be directly killed by aNK cells, and this cytotoxicity is increased by addition of mAb TRC105. These data suggest that activating ligands for NK-cell receptors as well as antigen targets for ADCC (CD105 and GD2) can contribute to aNK cell elimination of these TME cells. Thus, combining aNK cells with mAbs that target TME and tumor cells is a potentially effective immunotherapeutic strategy.

It has been reported that some tumor cell types express CD105, including breast and ovarian carcinomas, gastrointestinal stromal tumors, melanomas, and leukemias (37–41). The neuroblastoma cell line SH-SY5Y also has been reported to express CD105 (42). We found that CD105 was modestly expressed by neuroblastoma cell lines CHLA-255, CHLA-136, SMS-KCNR, and CHLA-90, but was not expressed by five others. Only CHLA-255 was significantly killed when ADCC against the CD105-positive cell lines was evaluated. These data do not support CD105 as an important target on neuroblastoma cells.

We developed a model in NSG mice, which lack T, B, and NK cells, to evaluate the impact of eliminating MSCs, monocytes/macrophages, and endothelial cells in the TME on the efficacy of therapy with aNK cells and dinutuximab against human neuroblastomas. This model is relevant to treatment of minimal disease because therapy began either three or four days after tumor cell injection when bulk disease and overt metastases were not yet detectable. This model utilizes human MSCs and monocytes coinjected with neuroblastoma cell lines or a PDX under the kidney capsule of NSG mice. The two human neuroblastoma cell lines and the PDX were derived from highly aggressive and drug-resistant metastatic tumors. One cell line (CHLA-255) expresses c-Myc protein, representing those patients with neuroblastoma whose high tumor expression of c-Myc is associated with a poor prognosis (43). Another (CHLA-136) has MYCN gene amplification, which causes high expression of the corresponding protein and which is an adverse prognostic factor (44). The PDX (COG-N-415x) has mutated *ALK* and amplified *MYCN*, both of which contribute to aggressive tumor behavior (45). Mice were treated with mAbs that are in clinical use and with aNK cells that are propagated and activated *ex vivo* similarly to currently

open clinical trials employing adoptive NK-cell therapy (NCT01729091, NCT01619761, NCT01787474, NCT01904136, NCT01823198, NCT02271711, NCT02280525), including a New Approaches to Neuroblastoma Therapy (NANT) consortium trial for neuroblastoma (NCT02573896). Thus, our model tests variables relevant to treatment of high-risk neuroblastoma in patients.

Our data show for the first time that antitumor immunotherapy of high-risk neuroblastomas with dinutuximab and aNK cells is improved by concurrently depleting MSCs, endothelial cells, and macrophages in the TME with anti-CD105 mAbs. Although mechanism(s) whereby depletion of these cells renders neuroblastoma cells more sensitive to dinutuximab and aNK cells are not yet fully understood, this could relate to decreased production of immunosuppressive and protumor cytokines, which is supported by our coculture experiments. Second, the marked decrease of vasculature in neuroblastomas by anti-CD105 mAbs combined with aNK cells could be another antitumor mechanism. Third, depletion of mouse macrophages could contribute to improved treatment with dinutuximab and aNK cells. Depletion of mouse macrophages may be due to targeting of CD105 on murine TAMs (46, 47) and/or to decreasing human chemoattractant and survival cytokines MCP-1, MCP-3, and CSF-1 produced in the TME. It has been reported that human MCP-1, MCP-3 and CSF-1 are cross-reactive with the receptors for their murine counterparts, and so the human cytokines may have recruited mouse monocyte/macrophages and supported their survival and activation in the human tumor xenografts (48, 49). We have shown that macrophages induce c-Myc expression and phosphorylation of STAT3 in neuroblastoma cells in syngeneic transplantable tumors, promoting neuroblastoma growth (50). Given the limited expression of CD105 on neuroblastoma cell lines and the PDX examined here, the direct targeting of neuroblastoma cells by anti-CD105 mAbs likely will not improve treatment with dinutuximab and aNK cells *in vivo*. Indeed, only one of three neuroblastoma cell lines (CHLA-255) was sensitive *in vitro* to ADCC mediated by TRC105 and aNK cells (Supplementary Fig. S6B and S6C). Overall, the efficacy of anti-CD105 mAbs in our neuroblastoma models required concurrent targeting of tumor cells with dinutuximab, suggesting that the role of depleting CD105<sup>+</sup> cells in the TME is to enable ADCC against neuroblastoma cells.

Although our models investigated clinically applicable therapies for treating high-risk neuroblastoma, they could have limitations. First, the TME in our xenograft model of neuroblastoma includes a mixture of human and murine cells with decreasing persistence of normal human cells over time. Notably, the humanized IgG1 TRC105 antibody mediated ADCC with human aNK cells *in vitro* against human MSC, endothelial cells, and monocytes. *In vivo*, tumor growth was decreased by the combination of TRC105 and M1043 with aNK cells and dinutuximab, which correlated with decreased human MSCs and murine endothelial cells and macrophages. TRC105 recognizes murine CD105 (19, 20), and our data indicate that TRC105 was the primary effector antibody against both human and murine cells *in vivo* because the rat IgG1 anti-murine CD105 M1043 only decreased tumor growth at early time points and did not prolong survival when added to aNK cells and dinutuximab *in vivo*. Second, in our quantitation of MVD, tumors were excised from each treatment group when mice were sacrificed due to morbidity from tumor growth, and since different groups had different survival times after completion of therapy, the effect of decreasing

persistence of human aNK cells on the measured MVD is difficult to estimate. Third, effector and target cells were from unrelated donors and so do not model the binding of human leukocyte antigen (HLA) class I molecules by autologous inhibitory and activating killer cell immunoglobulin-like receptors (KIR). Importantly, NK cells can mediate ADCC against MLL gene–rearranged leukemia cells that express inhibitory KIRs (51), and aNK cells generated with K562-mbIL21 feeder cells, as performed in our study, are not inhibited by autologous KIR–ligand interaction (27). Another possible limitation is the absence of effector T cells. However, neuroblastoma cells express little or no MHC class I molecules to present peptides to effector T cells and have relatively few gene mutations to generate unique tumor-associated antigens/peptides that could be targets for cytotoxic T cells (52–54). Finally, evidence has not been obtained to date showing an adaptive T-cell immune response to human neuroblastoma (55). These potential limitations could be evaluated in fully immunocompetent mice with transgenic or transplantable syngeneic neuroblastoma tumors that express GD2 and that have the spectrum of oncogenic abnormalities associated with aggressive tumor behavior in humans, but such models are not currently available.

In summary, this study shows that anti-human CD105 mAb TRC105 mediates ADCC with aNK cells against MSCs, monocytes, and endothelial cells. Depletion of these cells from the TME by anti-CD105 mAbs increases the antitumor activity of dinutuximab plus aNK cells. These data suggest that treatment of patients with high-risk neuroblastoma with dinutuximab may be enhanced by concurrently reducing MSCs, TAMs, and endothelial cells in the TME with anti-CD105 mAb therapy. Our findings support future clinical testing of TRC105 in combination with dinutuximab in patients with high-risk neuroblastoma. They also suggest that therapy of other malignancies with antibodies

could be improved by elimination of CD105<sup>+</sup> cells in the tumor microenvironment.

### Disclosure of Potential Conflicts of Interest

C.P. Theuer has ownership interests (including patents) at TRACON Pharmaceuticals. R.C. Seeger reports receiving commercial research grants from TRACON Pharmaceuticals. No potential conflicts of interest were disclosed by the other authors.

### Authors' Contributions

**Conception and design:** H.-W. Wu, C.P. Theuer, R.C. Seeger

**Development of methodology:** H.-W. Wu, M.A. Sheard, Y.A. DeClerck, H. Shimada, R.C. Seeger

**Acquisition of data (provided animals, acquired and managed patients, provided facilities, etc.):** H.-W. Wu, M.A. Sheard, L. Blavier, H. Shimada, R.C. Seeger

**Analysis and interpretation of data (e.g., statistical analysis, biostatistics, computational analysis):** H.-W. Wu, M.A. Sheard, J. Malvar, G.E. Fernandez, H. Shimada, R. Sposto, R.C. Seeger

**Writing, review, and/or revision of the manuscript:** H.-W. Wu, M.A. Sheard, J. Malvar, Y.A. DeClerck, H. Shimada, C.P. Theuer, R. Sposto, R.C. Seeger

**Administrative, technical, or material support (i.e., reporting or organizing data, constructing databases):** H.-W. Wu, R.C. Seeger

**Study supervision:** H.-W. Wu, R.C. Seeger

### Acknowledgments

This work was supported in part by grant 5P01 CA81403 from the National Cancer Institute (to R.C. Seeger), a grant from the Nautica Malibu Triathlon (to R.C. Seeger), and a grant from TRACON Pharmaceuticals (to R.C. Seeger).

The costs of publication of this article were defrayed in part by the payment of page charges. This article must therefore be hereby marked *advertisement* in accordance with 18 U.S.C. Section 1734 solely to indicate this fact.

Received October 12, 2018; revised March 29, 2019; accepted April 26, 2019; published first May 8, 2019.

### References

1. Yu AL, Gilman AL, Ozkaynak MF, London WB, Kreissman SG, Chen HX, et al. Anti-GD2 antibody with GM-CSF, interleukin-2, and isotretinoin for neuroblastoma. *N Engl J Med* 2010;363:1324–34.
2. Wu ZL, Schwartz E, Seeger R, Ladisch S. Expression of GD2 ganglioside by untreated primary human neuroblastomas. *Cancer Res* 1986;46:440–3.
3. Hanahan D, Coussens LM. Accessories to the crime: functions of cells recruited to the tumor microenvironment. *Cancer Cell* 2012;21:309–22.
4. Poggi A, Musso A, Dapino I, Zocchi MR. Mechanisms of tumor escape from immune system: role of mesenchymal stromal cells. *Immunol Lett* 2014;159:55–72.
5. Spaggiari GM, Capobianco A, Abdelrazik H, Becchetti F, Mingari MC, Moretta L. Mesenchymal stem cells inhibit natural killer-cell proliferation, cytotoxicity, and cytokine production: role of indoleamine 2,3-dioxygenase and prostaglandin E2. *Blood* 2008;111:1327–33.
6. Johann PD, Vaegler M, Gieseke F, Mang P, Armeanu-Ebinger S, Kluba T, et al. Tumour stromal cells derived from paediatric malignancies display MSC-like properties and impair NK cell cytotoxicity. *BMC Cancer* 2010;10:501.
7. Hendry SA, Farnsworth RH, Solomon B, Achen MC, Stacker SA, Fox SB. The role of the tumor vasculature in the host immune response: implications for therapeutic strategies targeting the tumor microenvironment. *Front Immunol* 2016;7:621.
8. Puré E, Lo A. Can targeting stroma pave the way to enhanced antitumor immunity and immunotherapy of solid tumors? *Cancer Immunol Res* 2016;4:269–78.
9. Bergfeld SA, Blavier L, DeClerck YA. Bone marrow-derived mesenchymal stromal cells promote survival and drug resistance in tumor cells. *Mol Cancer Ther* 2014;13:962–75.
10. Wolfe AR, Trenton NJ, Debeb BG, Larson R, Ruffell B, Chu K, et al. Mesenchymal stem cells and macrophages interact through IL-6 to promote inflammatory breast cancer in pre-clinical models. *Oncotarget* 2016;7:82482–92.
11. Noy R, Pollard JW. Tumor-associated macrophages: from mechanisms to therapy. *Immunity* 2014;41:49–61.
12. Song L, Asgharzadeh S, Salo J, Engell K, Wu HW, Sposto R, et al. Valpha24-invariant NKT cells mediate antitumor activity via killing of tumor-associated macrophages. *J Clin Invest* 2009;119:1524–36.
13. Asgharzadeh S, Salo JA, Ji L, Oberthuer A, Fischer M, Berthold F, et al. Clinical significance of tumor-associated inflammatory cells in metastatic neuroblastoma. *J Clin Oncol* 2012;30:3525–32.
14. Seon BK, Haba A, Matsuno F, Takahashi N, Tsujie M, She X, et al. Endoglin-targeted cancer therapy. *Curr Drug Deliv* 2011;8:135–43.
15. Dominici M, Le Blanc K, Mueller I, Slaper-Cortenbach I, Marini F, Krause D, et al. Minimal criteria for defining multipotent mesenchymal stromal cells. The International Society for Cellular Therapy position statement. *Cytotherapy* 2006;8:315–7.
16. Borriello L, Nakata R, Sheard MA, Fernandez GE, Sposto R, Malvar J, et al. Cancer-associated fibroblasts share characteristics and pro-tumorigenic activity with mesenchymal stromal cells. *Cancer Res* 2017;77:5142–57.
17. Paauwe M, Heijkants RC, Oudt CH, van Pelt GW, Cui C, Theuer CP, et al. Endoglin targeting inhibits tumor angiogenesis and metastatic spread in breast cancer. *Oncogene* 2016;35:4069–79.
18. Lastres P, Bellon T, Cabanas C, Sanchez-Madrid F, Acevedo A, Gougos A, et al. Regulated expression on human macrophages of endoglin, an Arg-Gly-Asp-containing surface antigen. *European J Immunol* 1992;22:393–7.

19. Uneda S, Toi H, Tsujie T, Tsujie M, Harada N, Tsai H, et al. Anti-endoglin monoclonal antibodies are effective for suppressing metastasis and the primary tumors by targeting tumor vasculature. *Int J Cancer* 2009;125:1446–53.
20. Tabata M, Kondo M, Haruta Y, Seon BK. Antiangiogenic radioimmunotherapy of human solid tumors in SCID mice using (125)I-labeled anti-endoglin monoclonal antibodies. *Int J Cancer* 1999;82:737–42.
21. Karzai FH, Apolo AB, Cao L, Madan RA, Adelberg DE, Parnes H, et al. A phase I study of TRC105 anti-endoglin (CD105) antibody in metastatic castration-resistant prostate cancer. *BJU Int* 2015;116:546–55.
22. Duffy AG, Ulahannan SV, Cao L, Rahma OE, Makarova-Rusher OV, Kleiner DE, et al. A phase II study of TRC105 in patients with hepatocellular carcinoma who have progressed on sorafenib. *United European Gastroenterol J* 2015;3:453–61.
23. Rosen LS, Hurwitz HI, Wong MK, Goldman J, Mendelson DS, Figg WD, et al. A phase I first-in-human study of TRC105 (Anti-Endoglin Antibody) in patients with advanced cancer. *Clin Cancer Res* 2012;18:4820–9.
24. Solari V, Borriello L, Turcatel G, Shimada H, Sposto R, Fernandez GE, et al. MYCN-dependent expression of sulfatase-2 regulates neuroblastoma cell survival. *Cancer Res* 2014;74:5999–6009.
25. Thompson PM, Maris JM, Hogarty MD, Seeger RC, Reynolds CP, Brodeur GM, et al. Homozygous deletion of CDKN2A (p16INK4a/p14ARF) but not within 1p36 or at other tumor suppressor loci in neuroblastoma. *Cancer Res* 2001;61:679–86.
26. Tran HC, Wan Z, Sheard MA, Sun J, Jackson JR, Malvar J, et al. TGFbeta1 blockade with galunisertib (LY2157299) enhances anti-neuroblastoma activity of the anti-GD2 antibody dinutuximab (ch14.18) with natural killer cells. *Clin Cancer Res* 2017;23:804–13.
27. Denman CJ, Senyukov VV, Somanchi SS, Phatarpekar PV, Kopp LM, Johnson JL, et al. Membrane-bound IL-21 promotes sustained *ex vivo* proliferation of human natural killer cells. *PLoS One* 2012;7:e30264.
28. Liu Y, Wu HW, Sheard MA, Sposto R, Somanchi SS, Cooper LJ, et al. Growth and activation of natural killer cells *ex vivo* from children with neuroblastoma for adoptive cell therapy. *Clin Cancer Res* 2013;19:2132–43.
29. Xu Y, Sun J, Sheard MA, Tran HC, Wan Z, Liu WY, et al. Lenalidomide overcomes suppression of human natural killer cell anti-tumor functions by neuroblastoma microenvironment-associated IL-6 and TGFbeta1. *Cancer Immunol Immunother* 2013;62:1637–48.
30. Weidner N, Semple JP, Welch WR, Folkman J. Tumor angiogenesis and metastasis—correlation in invasive breast carcinoma. *N Engl J Med* 1991;324:1–8.
31. Weidner N, Folkman J, Pozza F, Bevilacqua P, Allred EN, Moore DH, et al. Tumor angiogenesis: a new significant and independent prognostic indicator in early-stage breast carcinoma. *J Natl Cancer Inst* 1992;84:1875–87.
32. Patterson DM, Shohet JM, Kim ES. Preclinical models of pediatric solid tumors (neuroblastoma) and their use in drug discovery. *Current Protoc Pharmacol* 2011;Chapter 14:Unit 14.
33. Zhang T, Lee YW, Rui YF, Cheng TY, Jiang XH, Li G. Bone marrow-derived mesenchymal stem cells promote growth and angiogenesis of breast and prostate tumors. *Stem Cell Res Ther* 2013;4:70.
34. Ara T, Nakata R, Sheard MA, Shimada H, Buettner R, Groshen SG, et al. Critical role of STAT3 in IL-6-mediated drug resistance in human neuroblastoma. *Cancer Res* 2013;73:3852–64.
35. Martinez C, Hofmann TJ, Marino R, Dominici M, Horwitz EM. Human bone marrow mesenchymal stromal cells express the neural ganglioside GD2: a novel surface marker for the identification of MSCs. *Blood* 2007;109:4245–8.
36. De Giorgi U, Cohen EN, Gao H, Mego M, Lee BN, Lodhi A, et al. Mesenchymal stem cells expressing GD2 and CD271 correlate with breast cancer-initiating cells in bone marrow. *Cancer Biol Ther* 2011;11:812–5.
37. Henry LA, Johnson DA, Sarrio D, Lee S, Quinlan PR, Crook T, et al. Endoglin expression in breast tumor cells suppresses invasion and metastasis and correlates with improved clinical outcome. *Oncogene* 2011;30:1046–58.
38. Ziebarth AJ, Newshean S, Steg AD, Shah MM, Katre AA, Dobbin ZC, et al. Endoglin (CD105) contributes to platinum resistance and is a target for tumor-specific therapy in epithelial ovarian cancer. *Clin Cancer Res* 2013;19:170–82.
39. Gromova P, Rubin BP, Thys A, Cullus P, Erneux C, Vanderwinden JM. ENDOGLIN/CD105 is expressed in KIT positive cells in the gut and in gastrointestinal stromal tumours. *J Cell Mol Med* 2012;16:306–17.
40. Dolinsek T, Sersa G, Prosen L, Bosnjak M, Stimac M, Razborssek U, et al. Electrotransfer of plasmid DNA encoding an anti-mouse endoglin (CD105) shRNA to B16 melanoma tumors with low and high metastatic potential results in pronounced anti-tumor effects. *Cancers* 2015;8:p11: E3.
41. Dourado KMC, Baik J, Oliveira VKP, Beltrame M, Yamamoto A, Theuer CP, et al. Endoglin: a novel target for therapeutic intervention in acute leukemias revealed in xenograft mouse models. *Blood* 2017;129:2526–36.
42. Fang WH, Ahmed M, Wang Q, Li HM, Kumar P, Kumar S. PAX3 promotes tumor progression via CD105 signaling. *Microvasc Res* 2013;86:42–3.
43. Wang LL, Teshiba R, Ikegaki N, Tang XX, Naranjo A, London WB, et al. Augmented expression of MYC and/or MYCN protein defines highly aggressive MYC-driven neuroblastoma: a Children's Oncology Group study. *Br J Cancer* 2015;113:57–63.
44. Seeger RC, Brodeur GM, Sather H, Dalton A, Siegel SE, Wong KY, et al. Association of multiple copies of the N-myc oncogene with rapid progression of neuroblastomas. *N Engl J Med* 1985;313:1111–6.
45. De Brouwer S, De Preter K, Kumps C, Zabrocki P, Porcu M, Westerhout EM, et al. Meta-analysis of neuroblastomas reveals a skewed ALK mutation spectrum in tumors with MYCN amplification. *Clin Cancer Res* 2010;16:4353–62.
46. Ojeda-Fernández L, Recio-Poveda L, Aristorena M, Lastres P, Blanco FJ, Sanz-Rodríguez F, et al. Mice lacking endoglin in macrophages show an impaired immune response. *PLoS Genet* 2016;12:e1005935.
47. Aristorena M, Blanco FJ, de Las Casas-Engel M, Ojeda-Fernandez L, Gallardo-Vara E, Corbi A, et al. Expression of endoglin isoforms in the myeloid lineage and their role during aging and macrophage polarization. *J Cell Sci* 2014;127:2723–35.
48. Luini W, Sozzani S, Van Damme J, Mantovani A. Species-specificity of monocyte chemotactic protein-1 and -3. *Cytokine* 1994;6:28–31.
49. Manz MG. Human-hemato-lymphoid-system mice: opportunities and challenges. *Immunity* 2007;26:537–41.
50. Hadjidaniel MD, Muthugounder S, Hung LT, Sheard MA, Shirinbak S, Chan RY, et al. Tumor-associated macrophages promote neuroblastoma via STAT3 phosphorylation and up-regulation of c-MYC. *Oncotarget* 2017;8:91516–29.
51. Chan WK, Kung Sutherland M, Li Y, Zalevsky J, Schell S, Leung W. Antibody-dependent cell-mediated cytotoxicity overcomes NK cell resistance in MLL-rearranged leukemia expressing inhibitory KIR ligands but not activating ligands. *Clin Cancer Res* 2012;18:6296–305.
52. Pugh TJ, Morozova O, Attiyeh EF, Asgharzadeh S, Wei JS, Auclair D, et al. The genetic landscape of high-risk neuroblastoma. *Nat Genet* 2013;45:279–84.
53. Main EK, Lampson LA, Hart MK, Kornbluth J, Wilson DB. Human neuroblastoma cell lines are susceptible to lysis by natural killer cells but not by cytotoxic T lymphocytes. *J Immunol* 1985;135:242–6.
54. Prigione I, Corrias MV, Airolidi I, Raffaghello L, Morandi F, Bocca P, et al. Immunogenicity of human neuroblastoma. *Ann N Y Acad Sci* 2004;1028:69–80.
55. Majzner RG, Heitzeneder S, Mackall CL. Harnessing the immunotherapy revolution for the treatment of childhood cancers. *Cancer Cell* 2017;31:476–85.
56. Paaauw M, Schoonderwoerd MJ, Helderman R, Harryvan TJ, Groenewoud A, van Pelt GW, et al. Endoglin expression on cancer-associated fibroblasts regulates invasion and stimulates colorectal cancer metastasis. *Clin Cancer Res* 2018.

# Clinical Cancer Research

## Anti-CD105 Antibody Eliminates Tumor Microenvironment Cells and Enhances Anti-GD2 Antibody Immunotherapy of Neuroblastoma with Activated Natural Killer Cells

Hong-Wei Wu, Michael A. Sheard, Jemily Malvar, et al.

*Clin Cancer Res* 2019;25:4761-4774. Published OnlineFirst May 8, 2019.

**Updated version** Access the most recent version of this article at:  
doi:[10.1158/1078-0432.CCR-18-3358](https://doi.org/10.1158/1078-0432.CCR-18-3358)

**Supplementary Material** Access the most recent supplemental material at:  
<http://clincancerres.aacrjournals.org/content/suppl/2019/05/08/1078-0432.CCR-18-3358.DC1>

**Cited articles** This article cites 54 articles, 19 of which you can access for free at:  
<http://clincancerres.aacrjournals.org/content/25/15/4761.full#ref-list-1>

**Citing articles** This article has been cited by 4 HighWire-hosted articles. Access the articles at:  
<http://clincancerres.aacrjournals.org/content/25/15/4761.full#related-urls>

**E-mail alerts** [Sign up to receive free email-alerts](#) related to this article or journal.

**Reprints and Subscriptions** To order reprints of this article or to subscribe to the journal, contact the AACR Publications Department at [pubs@aacr.org](mailto:pubs@aacr.org).

**Permissions** To request permission to re-use all or part of this article, use this link  
<http://clincancerres.aacrjournals.org/content/25/15/4761>.  
Click on "Request Permissions" which will take you to the Copyright Clearance Center's (CCC) Rightslink site.